Coil Size and Long Range Excimers. 2. Good Solvent/ Nonsolvent Mixtures

M. Reyes Vigil

Departamento de Ingeniería, Escuela Politécnica, Universidad Carlos III, Leganes, 28911 Madrid, Spain

Carmen S. Renamayor and Inés F. Piérola*

Departamento de Química Física, Facultad de Ciencias, UNED, 28040 Madrid, Spain

Received February 20, 1995; Revised Manuscript Received May 24, 1995[⊗]

ABSTRACT: This paper presents results of steady state fluorescence spectra measurements on polyindene (PIN) and polyacenaphthylene (PAN) samples of different molecular weights, in dilute solution at constant temperature, 25 °C. Solvents were prepared by mixing a solvent and a precipitant in different proportions. Large changes in the size of the particles in solution (determined by turbidimetric methods) caused by incipient phase separation were necessary to produce significant changes of the excimer to monomer fluorescence ratio for both PIN and PAN. A linear relationship between the excimer to monomer fluorescence ratio and the volume of the polymer aggregates is found. Such a relationship is solvent viscosity independent. Several conclusions are drawn about the phase separation process in very dilute polymer solutions.

Introduction

Excimer formation in fluid media requires a conformational transition which must take place in the nanosecond time scale. Advantage may be taken of this phenomenon for the study of segmental mobility in polymeric systems.[1] Excimers formed through conformational transitions produced by rotation[2,3] are termed short range excimers (SRE).[2]

Some polymers like polyindene (PIN) and polyacenaphthylene (PAN) have the chromophore anchored by two points[4] to the chain backbone. It was initially proposed that PIN and PAN might not form SRE because neighbor monomeric units would have their chromophores not overlapping but on line.[5a] Nevertheless simulation experiments have demonstrated[5b] that, for PAN oligomers, in particular for syndiotactic oligomers, chromophores belonging to neighbor monomeric units may have significant overlap and therefore SRE may also be formed in PAN. It has been proposed that excimers in these polymers are formed by segmental diffusion[4-7] and are appropriately named long range excimers (LRE). Energy migration also plays an important role in excimer formation, since photon diffusion through the chain competes with segmental diffusion.[8] Isolated chromophores unable to form excimers and ground state preformed dimers have also been detected for PAN.[9]

Some copolymers may also form LRE.[10,11] A particular case are end to end excimers.[12] Intramolecular monomer concentration, which is inversely proportional to coil size, determines, together with solvent viscosity, the extent and rate of LRE formation.[8,11] It has also been found that the presence of a distribution of chain molecular weights and the excimer stability influences the diffusion-controlled long range excimer formation process.[13]

In a previous paper,[9] the dependence of LRE formation in PAN solution on several variables was analyzed. Coil size changes were produced[9] by dissolving PAN in mixtures of different compositions of two good solvents. Larger changes can be produced, at constant temperature, by mixing good and nonsolvents to produce a coil size decreasing from an expanded form to the unperturbed dimensions in θ conditions. Below θ conditions, with solvent compositions richer in nonsolvent than in the θ mixture (at the temperature of the experiment), there can be a contraction of the individual coils or aggregation of different coils. Collapse, via coil concentration, is unexpected in a low molecular weight sample,[14] and coil aggregation can be produced with consequent intermolecular excimer formation.[13] In this way we intend to analyze the phase separation process through measurements of monomer and excimer emissions of PIN and PAN dissolved in various good solvent/nonsolvent mixtures.

The size of polymer isolated coils in solvent–solvent mixtures can be determined by means of intrinsic viscosity measurements, but this technique cannot be applied to systems with extensive polymer aggregation. To determine the volume of the particles formed by chain aggregation a turbidimetric technique[15] is employed. Results from the excimer/monomer emission studies will be correlated with turbidimetric measurements.

Intermolecular excimers have been used to study phase separations in polymer blends.[16] They have also been applied to determine critical concentrations for chain overlap,[17] to study polymer aggregation processes driven by hydrophobic interactions,[18] and to analyze the influence of excluded volume effects on chain-to-chain interdiffusion.[19] In this paper we intend to analyze the dependence of the intermolecular excimer formation on the volume of the aggregated particles formed in the phase separation process of polymer/solvent/solvent ternary systems at constant temperature.

Experimental Section

Polymer samples were synthesized by cationic polymerization (PINC20[4] and PANL[20]) and electropolymerization (PINE2[4] and PANE1[4]). PANA was purchased from Aldrich and was twice reprecipitated on methanol from chloroform solution. Table 1 shows the molecular weight and polydispersity of the samples investigated. Solvents used in fluorescence measurements were purchased from Carlo Erba. They showed no

[⊗] Abstract published in *Advance ACS Abstracts,* July 1, 1995.

0024-9297/95/2228-5745$09.00/0 © 1995 American Chemical Society

Table 1. Characteristics of the Samples Here Studied

sample	$10^{-3} M_w$	M_w/M_n
PINC20	291	1.9
PINE2	2.3	2
PANL	140	1.44
PANA	5.8	1.36
PANE1	2.3	1.45

Table 2. Solvent Viscosity and Polymer Segmental Density at 25.0 °C, in the Pure Component 1 of the Solvent Mixtures Here Employed

solvent 1	solvent 2	η_1 (cP)	η_2 (cP)	PANL M/V (g/dL)	PINC20 M/V (g/dL)
THF	MeOH	0.47	0.55	3.35	1.45
Bz	MeOH	0.60	0.55	11.3	
Dx	MeOH	1.17	0.55	10.1	2.14
Bz	DEE	0.60	0.22	11.3	

emission under the constraints of the experimental conditions employed.

Emission spectra were recorded on a Hitachi F4000 fluorometer at constant temperature, 25 °C. The excitation wavelength was 280 nm for PAN and 270 nm for PIN samples. The absorbance at the excitation wavelength was always below 0.4, which corresponds to polymer concentrations 10^{-4} M, below the critical value for coil overlap. This makes it unlikely that intermolecular chain contacts will occur in the solutions in solvent/nonsolvent mixtures with compositions that do not exhibit phase separation. On the other hand, the low absorbance of the samples prevents autoabsorption or an inner-filter effect.

Aerated solutions were employed in each case since nitrogen purging does not modify significantly the fluorescence spectra of PIN, but increases appreciably the fluorescence ratio of PAN solutions. Polymer solutions in various solvent mixtures were employed without bubbling in order to get more reproducible compositions. All samples were prepared independently by adding the same volume of a polymer solution in the good solvent and aliquots of the good solvent and nonsolvent to always obtain the same final volume with different solvent mixture compositions.

The spectral overlap between monomer and excimer was considered negligible for PAN, but it was necessary to make a correction for PIN. From the shape of the pure monomer and excimer bands of PIN, it was found that I_M and I_E must be calculated from the intensities measured at 293 and 323 nm (I_{293} and I_{323}, respectively) as follows

$$I_E = I_{323} - 0.373 I_{293}$$

$$I_M = I_{293} - 0.117 I_{323}$$

The excimer to monomer fluorescence ratios of PAN samples were calculated as the ratio of the emission intensities measured at 400 and 342 nm (excimer and monomer band peaks, respectively).

Viscosities of solvent mixtures and polymer solutions were measured with an Ubbelohde modified viscometer fit in a Lauda Viscoboy automatic viscometer. The temperature was maintained at 25.00 ± 0.05 °C. Table 2 shows the intracoil segmental density (M/V where M and V represent the average molecular weight and volume of the polymer coils, respectively) of PINC20 and PANL in the good solvent. M/V is taken proportional to $[\eta]^{-1}$. Solvent viscosities[21] are also shown in Table 2.

Turbidimetric measurements were performed on a Perkin-Elmer Lambda 6 spectrophotometer. The turbidity at wavelength λ was calculated from the corresponding transmittance T by means of the equation

$$\tau(\lambda) = -(\ln T(\lambda))/l \qquad (1)$$

where l represents the optical path length, 1 cm in our case. Plots of τ vs λ^{-4} are linear for the range of wavelengths where there is no absorption of light: 420–500 nm for PAN and 330–500 nm for PIN solutions. In accordance with Mie theory (see ref 15 and references therein), the slope, S, of such plots is

$$S = \frac{24\pi^3 Vc}{d}\left(\frac{n^2-1}{n^2+1}\right)^2 {n_1}^4 \qquad (2)$$

where V, d, and c represent the weight average volume, the density, and the concentration in g/cm^3 of the scattering particles. n is the particle to solvent refractive index ratio and n_1 is the solvent refractive index. The density and refractive index of the two polymers in bulk were measured picnometrically and with an Abbe refractometer. Results are $n = 1.69$ for PIN and 1.68 for PAN and $d = 1.06$ for PIN and 1.15 for PAN. Taking these values for polymers in bulk, it was implicitly assumed that polymer aggregates are unswollen and nondraining particles. n_1 were taken from the literature.[21,22]

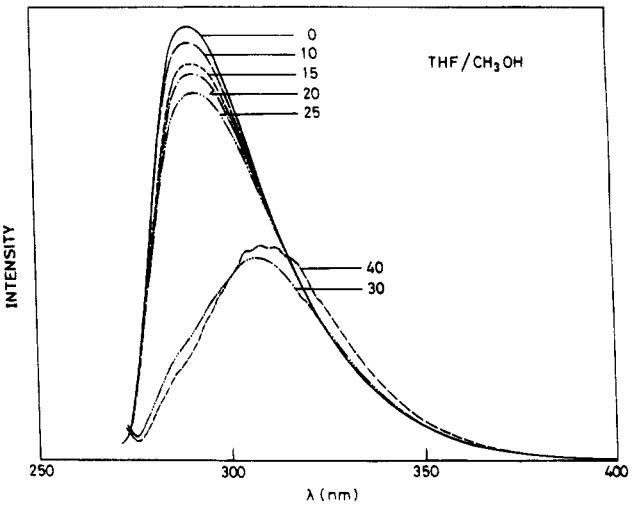

Figure 1. Fluorescence spectra of PIN dilute solutions in several THF–MeOH mixtures, at 25.0 °C. Φ_2 (%) is superimposed.

Results

Three regions can be observed in the fluorescence spectra of PIN and PAN, dissolved in good solvent (1)/nonsolvent (2) mixtures. In a certain range of solvent composition ranging from a pure good solvent ($\phi_2 = 0$) to a certain precipitant fraction that we call ϕ_2^s, the fluorescence ratio remains practically constant. In the second region with $\phi_2^s < \phi_2 < \phi_2^b$, the fluorescence ratio increases abruptly. Finally, with precipitant volume fractions larger than ϕ_2^b, the fluorescence ratio decreases or levels off. ϕ_2^s is determined at the point where the lines corresponding to the first and second regions intercept. Analogously, ϕ_2^b is determined in the intercept of the lines representing the second and third regions in Figure 2 and 3 (fluorescence measurements) or Figure 6 and 7 (turbidimetric measurements) type plots. ϕ_2^s and ϕ_2^b suggest the spinodal and binodal stages of phase separation in typical ternary systems.

Polyindene Fluorescence Spectra. Figure 1 shows the fluorescence spectra of PIN in solvent/nonsolvent mixtures of different compositions. The monomer emission of a high molecular weight sample is replaced by the excimer emission upon the addition of the nonsolvent. Very small changes are observed in the shape of the fluorescence spectra of a low molecular weight sample, but the total intensity decreases remarkably. Figure 2 depicts the dependence of the fluorescence ratio of two PIN samples on the volume fraction of nonsolvent in the solvent mixtures of tetrahydrofuran and methanol (THF–MeOH) and of dioxane with methanol (Dx–

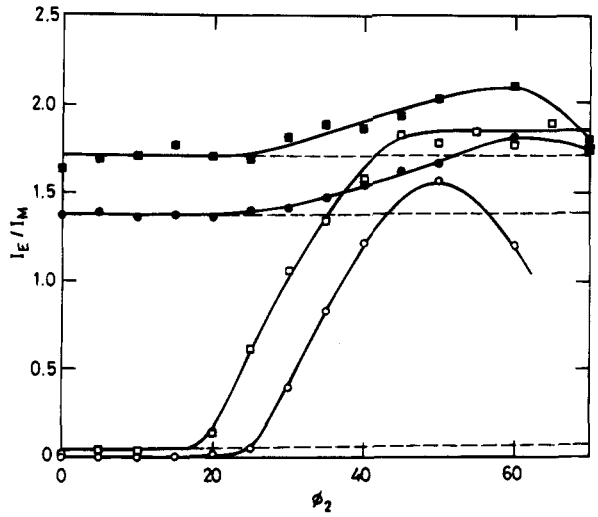

Figure 2. Fluorescence ratio of PIN dilute solutions at 25 °C in THF–MeOH (○) and Dx–MeOH (□) mixtures as a function of the volume fraction of precipitant. Empty points correspond to sample PINC20 and filled points to sample PINE2.

MeOH). Both mixtures have different viscosities (Table 2), and THF is[23] a better PIN solvent than Dx, but both mixtures show qualitatively the same behavior with the three regions mentioned above. The oligomer fluorescence ratio changes less than that of the high molecular weight sample, and it is interesting to notice that the maximum value is about the same for the two solvent mixtures and the two chain lengths. The basic photophysical features of PIN have been published elsewhere.[24]

Since solvent viscosity changes monotonously with ϕ_2, it must be concluded that the abrupt increase of the fluorescence ratio (second region) observed in Figure 2 is due to incipient phase separation. Polymer aggregation is expected for the mechanism of phase separation[14,25] in the range of molecular weights employed. Excimer forming sites (EFS) in a particle formed by aggregation of several polymer chains are both intra- and intermolecular, and thus the fluorescence ratio increases with respect to solutions with isolated coils. Apparently, the solution remains homogeneous and transparent without polymer precipitation even at compositions richer in nonsolvent than those corresponding to the transition. However, the descent of the fluorescence ratio with nonsolvent proportions larger than ϕ_2^b suggests that, progressively, polymer particles coalesce and precipitate to the bottom of the cell. The fluorescence ratio of the particles remaining in solution decreases after partial precipitation because particles remaining in solution are the smallest ones, those having a low aggregation number, and therefore fewer intermolecular excimers.

Table 3 summarizes the volume fraction of precipitant which delimits the second region (ϕ_2^s, ϕ_2^b) and the relative change of the fluorescence ratio (ΔFR) along the transition.

Polyacenaphthylene Fluorescence Spectra. The trend of the PAN fluorescence ratio plotted versus the nonsolvent volume fraction in the solvents mixture (Figure 3) is about the same as for PIN (Figure 2), but the changes are smaller.

The lower molecular weight samples show no change upon addition of nonsolvent or a much smaller increase of the fluorescence ratio which initiates at a larger proportion of nonsolvent ϕ_2^s (Table 3). Solvent thermodynamic quality also influences ϕ_2^s: for example, THF is[9] a better PAN solvent than benzene (Bz) and ϕ_2^s is larger for THF–MeOH than for Bz–MeOH, or MeOH is a worse PAN solvent than diethyl ether (DEE) and ϕ_2^s is smaller for Bz – MeOH than for Bz – DEE with the same polymer molecular weight. Changes of the fluorescence ratio along the transition are smaller for the better solvent (Table 3).

Table 3. Precipitant Volume Fraction of the Range of Compositions Corresponding to the Abrupt Change of the Fluorescence Ratio (FR) and the Slope (S) of the Turbidity Plots (Marked with *) and Relative Increment of Those Magnitudes along the Transition

polymer	solvent	$\phi_2^s - \phi_2^b$	Δ(FR)	$\Delta(S)$
PANL	Bz–Me OH	0.13 to >0.70	0.93	
PANL	THF–MeOH	0.17–0.65	0.73	
PANL	Bz–DEE	0.30 to >0.70	0.64	
		0.40–0.50*		7.6
PANA	Bz–MeOH	0.35–0.60	0.26	
PANA	Bz–DEE	0.35 to >0.70	0.06	
		0.35–0.40*		1.6
PANE1	Bz–MeOH	0.35 to >0.70	−0.07	
PINC20	Dx–MeOH	0.18 to >0.70	95.0	
		0.15–0.25*		45
PINC20	THF–MeOH	0.25–0.50	80.0	
		0.20–0.40*		55
PINE2	THF–MeOH	0.30–0.60	0.31	
PINE2	Dx–MeOH	0.25–0.60	0.24	

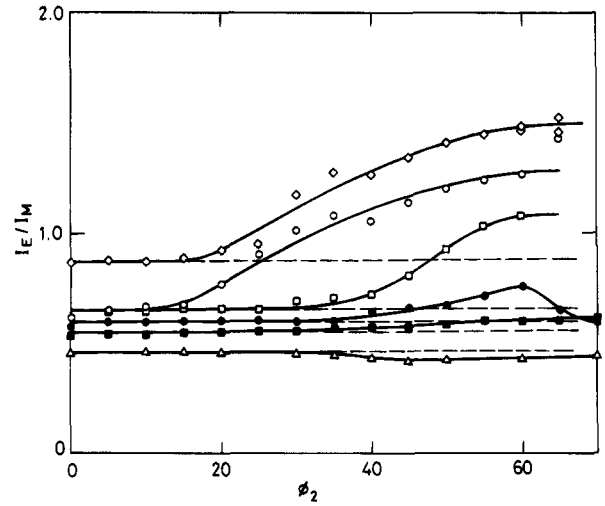

Figure 3. Fluorescence ratio of PAN dilute solutions at 25 °C in THF–MeOH (◇) Bz–MeOH (○), and Bz–DEE (□) mixtures as a function of the volume fraction of precipitant. Empty points correspond to sample PANL, filled points to sample PANA, and △ points to sample PANE1.

Excimer emission shifts to the blue for nonsolvent volume fractions larger than ϕ_2^s (Figure 4). This result suggests that intermolecular excimers formed in such polymer aggregates are less stable than intramolecular excimers because the overlap of aromatic rings is less efficient. Only an ordered structure of chains in PAN aggregates would explain how intramolecular long range excimers have different geometries than intermolecular excimers.

Turbidity Measurements. τ depends on λ^{-4}, and Figure 5 type plots allow us to determine S, a wavelength independent turbidity parameter which is directly proportional to the volume of the scattering particles V. The dependence of S (and therefore of V) on ϕ_2 is, qualitatively, the same as for the fluorescence ratio, with three well-defined regions. There is a range of solvent compositions with V about constant (Figure 6). ϕ_2^s is about the same for turbidity and fluorescence

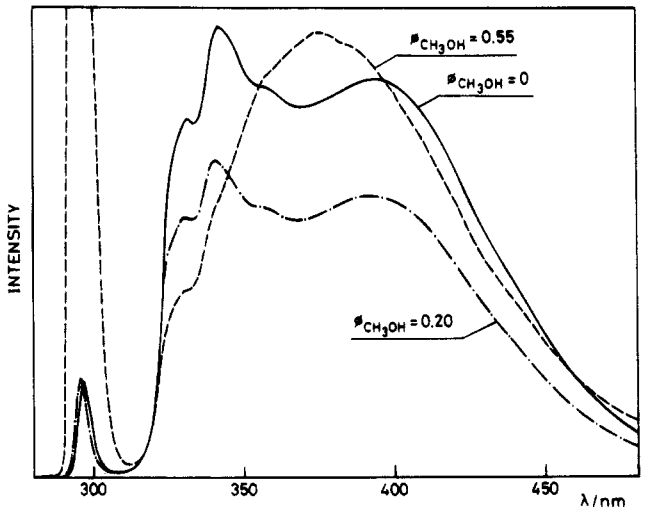

Figure 4. Fluorescence spectra of PAN dilute solutions in several Bz–MeOH mixtures, at 25 °C.

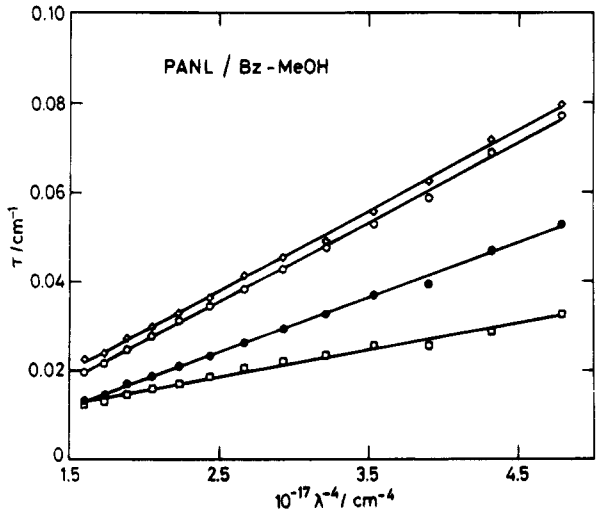

Figure 5. Turbidity plots for PANL in Bz–MeOH mixtures of different compositions (ϕ_2 (%): 0 (□), 35 (△), 40 (○), and 45 (●)).

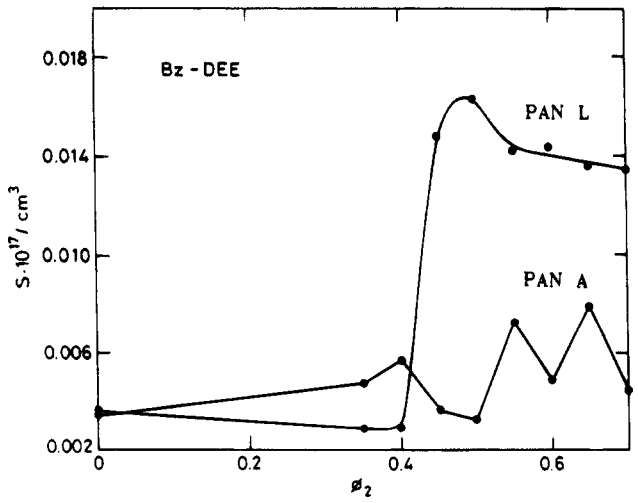

Figure 6. Slopes of the turbidity plots of PANL and PANA in Bz–DEE mixtures as a function of the volume fraction of precipitant.

measurements (Table 3). With solvent compositions in the range ϕ_2^s to ϕ_2^b, V increases (as the FR) to reach a maximum value at a ϕ_2^b smaller than for the FR (Table 3). This increment of V supports the idea of phase

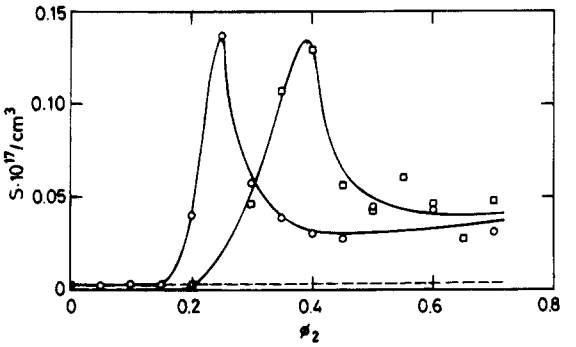

Figure 7. Slopes of the turbidity plots of PINC20 in THF–MeOH (□) and Dx–MeOH (○), as a function of the volume fraction of precipitant.

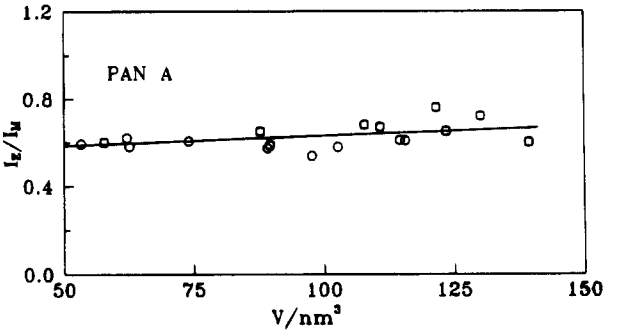

Figure 8. Fluorescence ratio of low molecular weight PAN as a function of the volume of the scattering particles in solution for two solvent mixtures. Symbols are the same as in previous figures.

separation through aggregation, consistent with the formation of intermolecular excimers as mentioned above. For solvent mixtures richer in nonsolvent ($\phi_2 > \phi_2^b$), V (see Figure 7 for PIN), as does the fluorescence ratio, decreases, supporting the idea that only the smallest particles remain in solution.

S of PAN (Table 3) increases by a factor of 2 for the low molecular weight sample and a factor of 8 for the largest molecular weight employed. These numbers provide some insight into the number of chains which form the aggregates. The number is much larger, about 50, for PIN samples depending on solvent quality. Nevertheless, the volume of the scattering particles is about the same for both polymers, ranging from 10 to 500 nm.[3] These volumes correspond to spheres with 1–5 nm radii for densely packed chains, assuming that their density is that for the bulk polymer.

Discussion

Figure 8–10 show the dependence of PIN and PAN fluorescence ratios on the volume of the scattering particles V for solvent compositions in the range ϕ_2^s to ϕ_2^b. The volume of the particles in solution of the low molecular weight PAN sample (Figure 8) increases slightly over this solvent composition range, but their fluorescence ratio changes only about 1×10^{-3} per nm^3, independent of the characteristics of the solvent mixture employed. For high molecular weight PAN, the fluorescence ratio changes by about 2×10^{-3} per nm^3 and can be also considered solvent independent (Figure 9). Given the spread of points in Figures 8 and 9, the difference of these two slopes is not significant.

For high molecular weight PIN (Figure 10), the fluorescence ratio also increases linearly with V and points corresponding to different solvent mixtures yield

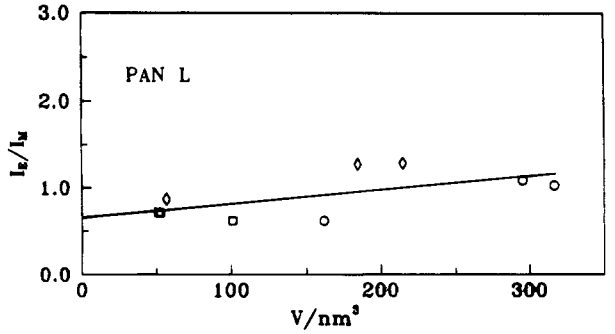

Figure 9. Fluorescence ratio of high molecular weight PAN as a function of the volume of the scattering particles in solution for three solvent mixtures. Symbols are the same as in previous figures.

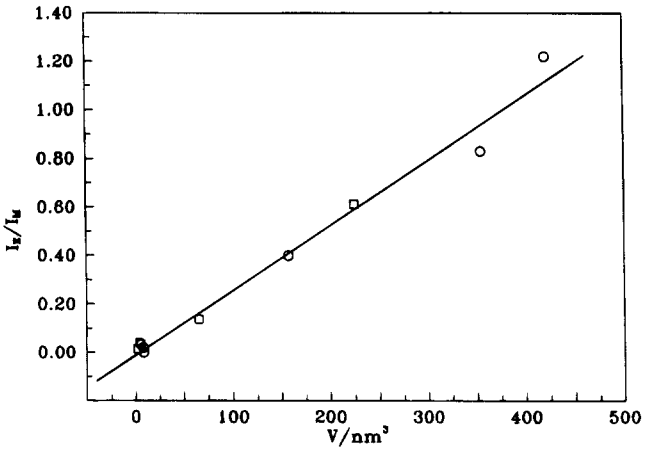

Figure 10. Fluorescence ratio of high molecular weight PIN as a function of the volume of the scattering particles in solution for two solvent mixtures. Symbols are the same as in previous figures.

the same line with a slope of 3.0×10^{-3} per nm^3. Since excimer formation in polymer aggregates does not depend on solvent viscosity, it means that solvent does not penetrate into the aggregates; in this way, polymer aggregates are densely packed, with the same microviscosity inside, independently of the solvent surrounding the polymer particles.

Differences between PIN and PAN may be due to the different mechanisms of excimer formation typical of these two polymers which were previously discussed.[4,6]

Thermally induced phase separation of two component mixtures has been studied extensively.[26] Two different mechanisms can be observed in the early stages, spinodal decomposition or nucleation and growth. In spinodal decomposition, phase separation occurs by an instantaneous and continuous process involving a diffusional flux against a concentration gradient to build progressively larger aggregation particles.[27] Less common is the nucleation and growth mechanism.[28] The same mechanisms should be expected in phase separation processes at constant temperature, with solvent/nonsolvent mixtures. In the systems studied herein, the solvent composition which initiates phase separation depends on the nature of the solvent/nonsolvent pair, but it cannot be discerned whether phase separation is a consequence of differences in viscosity, solvent thermodynamic quality, or both. Nevertheless, the Bz–MeOH and THF–MeOH mixtures have about the same viscosity, and ϕ_2^s for PAN is significantly larger for the THF mixture because it is a better solvent for PAN than Bz. This suggests that solvent viscosity plays a less important role than solvent thermodynamic quality, hence arguing against spinodal decomposition. Additional experimental work should be performed to clarify this point.

In a second stage of the phase separation process, in order to reduce the surface energy associated with interfacial area, the system evolves by reducing the number of polymer particles and increasing their size. This process is called coarsening.[29] In nonisopycnic systems gravitational sedimentation of large particles dominates this second stage of the phase separation. According to turbidimetric measurements, the phase separation process of PIN and PAN takes place over a narrow range of solvent compositions, about 10%. This suggests that it is a cooperative process, such that the particles formed in systems with composition ϕ_2^s favor the formation of larger particles which precipitate once they reach a maximum value at ϕ_2^b. Only kinetic studies of phase separation would yield information on the coarsening mechanism, but it is interesting to notice that independently of solvent viscosity, polymer particles of the same size are formed.

Acknowledgment. Financial support from DGICYT and CAM (Spain) under grants MAT93/0167 and 247/92 (respectively) and from the Acción Concertada Spain-Portugal (HP94/016) is gratefully acknowledged.

References and Notes

(1) Morawetz, H. In *Photophysical and Photochemical Tools in Polymer Science*; Winnik, M. A., Ed.; NATO ASI Series, Series C, Vol. 182; D. Reidel Publishing Co.: Dordrecht, Holland, 1985.
(2) Masegosa, R. M.; Hernández-Fuentes, I.; Piérola, I.; Horta, A. *Polymer* **1987**, *28*, 231.
(3) Salom, C.; Semlyen, J. A.; Clarson, S.; Hernández-Fuentes, I.; Maçanita, A.; Horta, A.; Piérola, I. F. *Macromolecules* **1991**, *24*, 6827.
(4) Renamayor, C. S.; Gómez-Antón, M. R.; Calafate, B.; Mano, E. B.; Radic, D.; Gargallo, L.; Freire, J. J.; Pierola, I. F. *Macromolecules* **1991**, *24*, 3328.
(5) (a) Wang, Y.-C.; Morawetz, H. *Makromol. Chem. Suppl.* **1975**, *1*, 283. (b) Mendicuti, F.; Kulkarni, R.; Patel, B.; Mattice, W. L. *Macromolecules* **1990**, *23*, 2560.
(6) Renamayor, C. S.; Gómez-Antón, M. R.; Piérola, I. F. *J. Appl. Polym. Sci. Polym. Symp.* **1990**, *45*, 317.
(7) (a) David, C.; Lempereur, M.; Geuskens, G. *Eur. Polym. J.* **1972**, *8*, 1019. (b) Reid, R. F.; Soutar, I. *J. Polym. Sci., Polym. Phys. Ed.* **1980**, *18*, 457.
(8) (a) Cabaness, W. R.; Lin, L.-Ch. *J. Polym. Sci., Polym. Chem. Ed.* **1984**, *22*, 857. (b) Anderson, R. A.; Reid, R. F.; Soutar, I. *Eur. Polym. J.* **1980**, *16*, 945. (c) Galli, G.; Solaro, R.; Chiellini, E.; Fernyhough, A.; Ledwith, A. *Macromolecules* **1983**, *16*, 502. (d) Ghiggino, K. P. *Makromol. Chem., Macromol. Symp.* **1992**, *53*, 355.
(9) Vigil, M. R.; Renamayor, C. S.; Piérola, I. F. *Macromolecules* **1994**, *27*, 2297.
(10) Holden, D. A.; Safarzadeh-Amiri, A.; Sloan, Ch. P.; Martin, P. *Macromolecules* **1987**, *20*, 807.
(11) Cuniberti, C.; Musi, L.; Perico, A. *J. Polym. Sci., Polym. Lett. Ed.* **1982**, *20*, 265.
(12) Li, X. B.; Winnik, M. A.; Guillet, J. E. *Macromolecules* **1983**, *16*, 992.
(13) Liu, G. *Macromolecules* **1993**, *26*, 6998.
(14) Flory, P. J. *Principles of Polymers Chemistry*; Cornell University Press: London: 1953.
(15) (a) Dorado, A. P.; Piérola, I. F.; Baselga, J.; Gargallo, L.; Radic, D. *Makromol. Chem.* **1989**, *190*, 2975. (b) Dorado, A. P.; Piérola, I. F.; Baselga, J.; Gargallo, L.; Radic, D. *Makromol. Chem.* **1990**, *191*, 2905.
(16) (a) Frank, C. W.; Gashgari, M. A.; Semerak, S. N. In *Photophysical and Photochemical Tools in Polymer Science*; Winnik, M. A., Ed.; NATO ASI Series, Series C, Vol. 182; D. Reidel Publishing Co., Dordrecht, Holland, 1985. (b) Dong, L.; Hill, D. J. T.; Whittaker, A. K.; Ghiggino, K. P. *Macromolecules* **1994**, *27*, 5912.

(17) (a) Roots, J.; Nystrom, B. *Eur. Polym. J.* **1979**, *15*, 1127. (b) Tsai, F. J.; Torkelson, J. M. *Polymer* **1988**, *29*, 1004.
(18) (a) Granville, M.; Jerome, R. J.; Teyssie, P.; Schryver, F. C. *Macromolecules* **1988**, *21*, 2894. (b) Winnik, F. M. *Chem. Rev.* **1993**, *93*, 587.
(19) Zanocco, G.; Abuin, E.; Lissi, E.; Gargallo. L.; Radic, D. *Eur. Polym. J.* **1982**, *18*, 1037.
(20) Leon, L. M.; Altuna, P.; Petter, D. C. *Eur. Polym. J.* **1980**, *16*, 929.
(21) Riddick, J. A.; Bunger, W. B.; Sakano, T. K. *Organic Solvents*, 4th ed.; Wiley: New York, 1986.
(22) *Polymer Handbook;* Brandrup, J., Immergut, E. H., Eds.; Wiley: New York, 1989.
(23) The Mark–Houwink parameters for PIN at 25 °C are $a = 0.57$ in tetrahydrofuran and $a = 0.54$ for dioxane.
(24) Renamayor, C. S.; Maçanita, A.; Gómez-Antón, M. R.; Piérola, I. F. Submitted for publication.
(25) Cuniberti, C.; Bianchi, U. *Polymer* **1974**, *15*, 346.
(26) Song, S. W.; Torkelson, J. M. *Macromolecules* **1994**, *27*, 6389.
(27) (a) de Gennes, P. G. *J. Chem. Phys.* **1980**, *72*, 4756. (b) Binder, K. *J. Chem. Phys.* **1983**, *79*, 6387.
(28) Krishnamurthy, S.; Bansil, R. *Phys. Rev. Lett.* **1983**, *50*, 2010.
(29) Aubert, J. H. *Macromolecules* **1990**, *23*, 1446.

MA950204D